



ELSEVIER

Analytica Chimica Acta 380 (1999) 303–310

ANALYTICA  
CHIMICA  
ACTA

## Infrared regular reflectance and transmittance instrumentation and standards at NIST

S.G. Kaplan<sup>\*</sup>, L.M. Hanssen

*Optical Technology Division, NIST, Gaithersburg, MD 20899, USA*

Received 17 June 1998; accepted 25 August 1998

### Abstract

Instrumentation is described that has been constructed at the National Institute of Standards and Technology (NIST) for the measurement of regular reflectance and transmittance over the 2–25  $\mu\text{m}$  wavelength region. This includes both specialized accessories used with Fourier-transform infrared (FT-IR) spectrometers and laser-based systems for high optical density transmittance measurements. The FT-IR systems have been used to develop standard reference materials for IR regular transmittance. © 1999 Published by Elsevier Science B.V. All rights reserved.

*Keywords:* Infrared regular reflectance; Transmittance; FT-IR measurements; Beam geometry

### 1. Introduction

The Optical Technology Division at NIST has developed Fourier-transform infrared (FT-IR) based instrumentation for accurate measurement of regular spectral transmittance ( $T$ ) and reflectance ( $R$ ) in the mid-IR wavelength region. Two commercial FT-IR spectrometers, a Bio-Rad FTS-60A and a Bomem DA3<sup>1</sup>, have been fitted with specialized accessories for  $T$  and  $R$  measurements. The Bio-Rad system, shown in Fig. 1, can be used to perform transmittance measurements in the standard  $f/3$  sample compartment

geometry, or  $T$  and  $R$  measurements with one of two external arrangements. A 6 in. diameter side-mount integrating sphere system can be used to perform absolute regular  $R$  and  $T$  measurements at  $8^\circ$  incidence on specular samples, with an  $f/4$  incident beam geometry [1]. A goniometer system has been constructed for polarized, angle-dependent measurements, and an optical access cryostat for 10–600 K operation can be used to control the sample temperature.

The Bomem DA3 is configured with an 8 in. center-mount integrating sphere, a high-temperature black-body source, and an additional cryostat [2] for  $T/R$  measurements from 10 to 77 K. A collimated beam transmittance accessory has also been added, and used to perform high-resolution measurements on etalon samples to measure the mid-IR index of refraction to  $10^{-4}$  uncertainty. In this paper we describe the investigation and reduction of radiometric error sources in the FT-IR measurements, results of inter-comparisons

<sup>\*</sup>Corresponding author. Tel.: +1-301-975-2366; fax: +1-301-869-5700; e-mail: simon.kaplan@nist.gov

<sup>1</sup>The use of certain trade names in this paper is for informational purposes only and does not constitute an endorsement by NIST that this equipment is necessarily the best suited for the task.

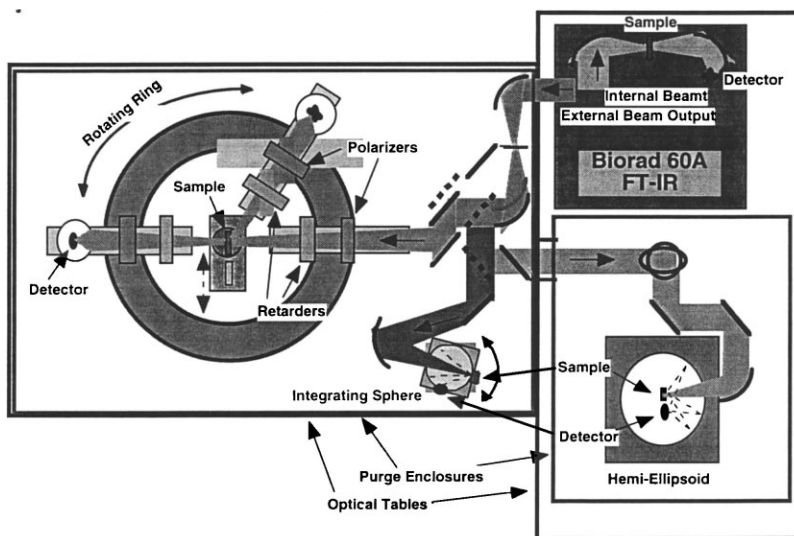


Fig. 1. Goniometer and integrating sphere systems with Bio-Rad FT-IR.

among FT-IR, grating monochromator, and laser-based systems, and the development of standard reference materials for regular IR transmittance.

FT-IR spectrometers are the most widely used instruments for routine IR  $T$  and  $R$  analysis of solid samples. Although they provide advantages in signal-to-noise ratio and wavelength accuracy over dispersive instruments, FT measurements are more prone to errors [3] due to inter-reflections [4,5], detector non-linearity and non-equivalence [6,7], and background thermal radiation [8,9]. We have found that it is possible to perform measurements of  $T$  and  $R$  with FT-IR instruments to within 0.2–1% relative uncer-

tainities, depending upon the sample and type of measurement [10].

## 2. Experimental

### 2.1. "Conventional" transmittance measurements

$T$  and  $R$  measurements are performed in several different configurations. For  $T$  measurements of fairly thin samples, which have a small effect on the beam geometry, a modified version of the standard sample compartment geometry is used [10], as shown in Fig. 2. Half-blocks made of IR absorbing black felt

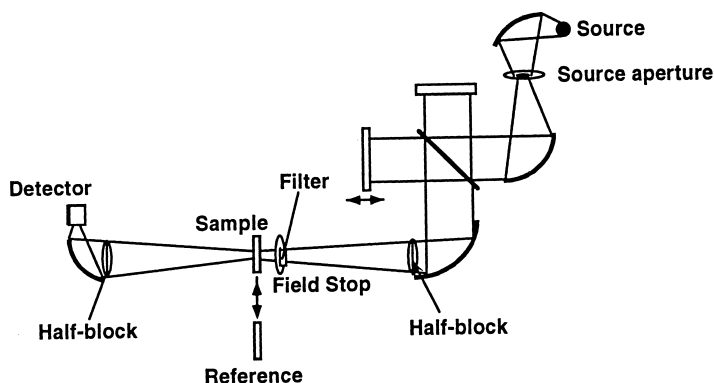


Fig. 2. Optical layout for FT-IR transmittance measurements as described in the text.

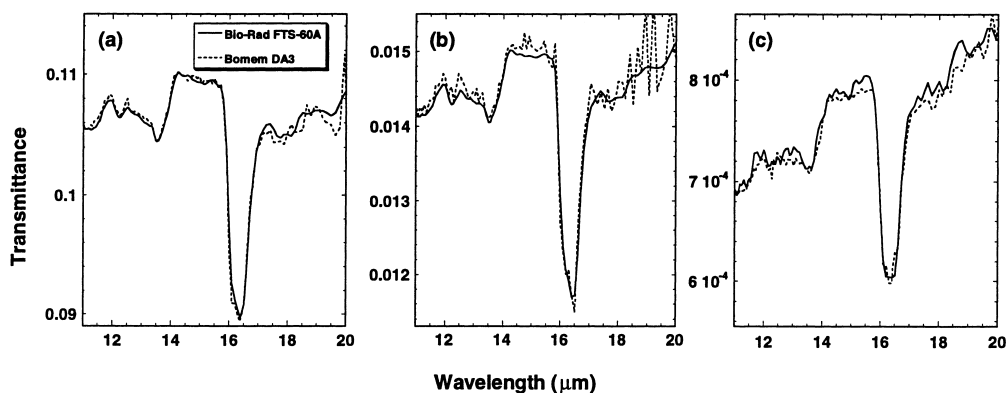


Fig. 3. Comparison between measurements of three different metal film/Si neutral density filters performed with two different FT-IR systems.

are used to eliminate inter-reflections among the sample, detector and interferometer. Neutral-density or band pass filters are placed (tilted, to avoid inter-reflections) before the sample position, or used as the reference for the transmittance calculation, in order to keep the detector response linear and equivalent between sample and reference. A field stop is placed just before the sample position to limit diffuse thermal radiation from the source aperture.

With the use of appropriate filters and detectors, it is possible to measure transmittances as low as  $10^{-6}$  with this configuration [11]. For optically thin ( $<1$  mm) samples with fairly neutral attenuation, the contributions of various error sources to the total radiometric uncertainty have been estimated [10]. Expanded ( $2\sigma$ ) relative uncertainties are in the range of 0.5–1% for samples with optical densities up to 3. These uncertainty estimates have been tested by inter-comparison between the two FT-IR systems and by inter-comparison with laser measurements on etalon-free samples.

Fig. 3 shows a comparison between transmittance measurements from 11 to 20  $\mu\text{m}$  on thin metal-coated Si samples with optical densities near 1, 2, and 3 made on the Bio-Rad and Bomem FT-IR spectrometers using the configuration shown in Fig. 2. Both systems were set up with a ceramic global source and KBr:Ge beamsplitter, and the spectral resolution was  $8\text{ cm}^{-1}$ . A 2 mm room temperature pyroelectric detector was used with the Bio-Rad, while a 1 mm 77 K mercury–cadmium–telluride (MCT) detector was used with the Bomem. The beam geometry at the sample position is

$f/3$  in the Bio-Rad and  $f/4$  in the Bomem. For the OD 1 ( $\text{OD} = -\log_{10} T$ ) sample in frame (a), the two measurements agree to within 0.5% over most of the region. For the higher OD samples shown in (b) and (c), the signal-to-noise ratio is lower, but the measurements still agree to within 1–2%. The OD 2 measurement was done with the OD 1 filter as a reference, while the OD 3 measurement was done with the OD 2 filter as a reference on the Bomem, and the OD 1 filter on the Bio-Rad.

Fig. 4 shows the results of an inter-comparison between two laser transmittance measurements at 3.39  $\mu\text{m}$  and 10.6  $\mu\text{m}$  and the FT-IR system on two metal film/Lexan filters [10]. The Lexan substrates are only 100 nm thick, allowing a direct comparison between the laser and FT-IR results without the complication of Fabry–Perot fringes in the spectra. In this case it can be seen that the two sets of measurements agree to within 0.5–1%, within the expanded uncertainty of the laser measurements.

## 2.2. *T/R measurements with integrating sphere*

For the measurement of absolute specular reflectance, there are two external arrangements, as shown in Fig. 1. The integrating sphere system, described in the preceding paper [12], can be used to perform either *T* or *R* measurements at  $8^\circ$  incidence. By rotating the sphere about both the center and the sample position, it is possible to make either a sample or reference measurement in such a way that the incident beam

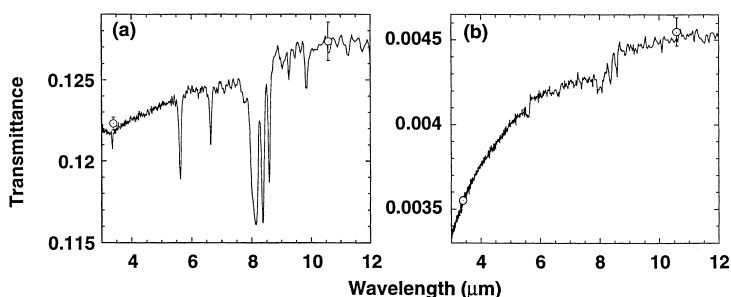


Fig. 4. Comparison between transmittances of two thin metal film/Lexan neutral density filters measured with an FT-IR system (lines) and laser systems at 3.39  $\mu\text{m}$  and 10.6  $\mu\text{m}$  (circles).

in the reference measurement strikes the surface of the sphere in an optically equivalent position to that of the specular beam from the sample. Thus the ratio of the two measurements provides an absolute measurement [1], independent of sphere throughput.

The high degree of uniformity of the sphere, combined with its averaging properties, greatly reduces the effects of the sample on the beam geometry at the position of the 6 mm MCT detector. The  $8^\circ$  incidence on the sample, with  $f/4$  geometry, eliminates inter-reflections with the interferometer, while the field stop at the focal position of the  $90^\circ$  off-axis parabolics limits diffuse source aperture radiation. The low throughput ( $\sim 0.5\%$ ) of the sphere tends to keep the detector response nearly linear for mid-IR measurements. Other sources of error in the measurement include

1. a small (ca. 0.1–0.2%) non-equivalence between the specular positions on the sphere wall opposite the sample and reference ports,
2. small ( $<1^\circ$ ) vertical misalignment between the transmittance and reflectance measurements,
3. light diffusely scattered by the sample,
4. light emitted from the sample and modulated by the interferometer before reaching the detector, and
5. overfilling of the sample/reference ports by scattered or diffracted incident light.

These effects can be characterized and approximately accounted for in the results [1].

Several measurements have been performed to test the accuracy of  $T$  and  $R$  values obtained with this integrating sphere system. Fig. 5 shows  $T$  and  $R$

measured for parallel-sided samples of ZnSe (thickness 3 mm) and Si (thickness 2 mm). In each case, there is a wavelength region in which the absorption coefficient is negligibly small ( $<10^{-3} \text{ cm}^{-1}$ ) [13], so that the measured absorbance,  $1-T-R$ , should be zero within the reproducibility of the experiment in the absence of the various errors listed above. As can be seen in this figure, the measured residual absorbance is typically less than 0.3% in these regions. Also shown are  $T$  and  $R$  curves calculated from tabulated values for the index of refraction of each material [14]. These calculations treat the multiple reflections in the sample incoherently, and include the measured degree of linear polarization of the incident beam, which is generally small ( $|s_1| < 0.07$ ) except near  $8 \mu\text{m}$ , where the  $p$ -polarized absorption in the  $\text{SiO}_x$  overcoating [15,16] on several of the Al mirrors gives  $s_1 \sim 0.5$  (these mirrors have since been replaced with Au-coated ones). The calculations are done for collimated light at  $8^\circ$  incidence; proper averaging over the range of incidence angles is expected to yield differences of less than 0.03%.

The good agreement between the expected values and the measured values tends to confirm that the  $T$  and  $R$  measurements with the sphere are accurate to within 0.3% for these samples, even with none of the corrections 1–5 listed above having been applied. The structure near  $6 \mu\text{m}$  in frames (a) and (c) is due to  $\text{H}_2\text{O}$  adsorbed in the sphere wall coating, which causes some variation in throughput as a function of input geometry. Dielectric samples such as these actually provide a more stringent test of the sphere uniformity than opaque front-surface reflectance samples, because the multiple reflections within the material

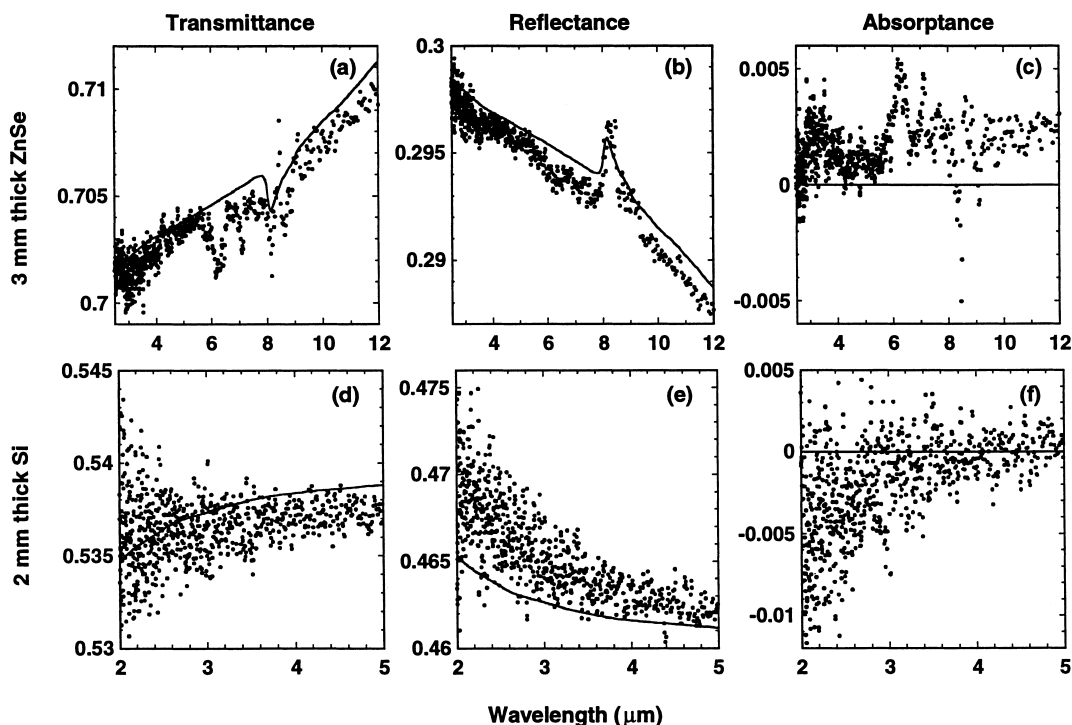


Fig. 5. Transmittance, reflectance and absorbance measured with an integrating sphere for a 3 mm thick piece of ZnSe (a,b,c) and a 2 mm thick piece of Si (d,e,f). In each frame the circles show the measured signal and the lines show the calculated signal using tabulated values for the index of refraction, as described in the text.

increase the size of the transmitted or reflected spot on the sphere wall compared to the reference spot. To test the accuracy for lower signal levels, an intercomparison with a “conventional” measurement was performed on the transmittance of an OD 2 filter such as that shown in Fig. 3(b), and the relative differences were found to be less than 1%.

An inter-comparison was made between the reflectance values of a gold mirror standard reference material measured on this sphere system and the NIST spectral tri-function absolute reference reflectometer (STARR) [17], which uses a grating monochromator and has a long-wavelength limit of 2.5  $\mu\text{m}$ . This comparison is shown in Fig. 6. In the region of overlap of the two sets of data (1.5–2.5  $\mu\text{m}$ ) the differences are less than 0.1%, which is within the estimated uncertainty ( $\pm 0.3\%$ ) of the STARR data. The structure near 8  $\mu\text{m}$  is again related to *s*-polarization of the beam coming from  $\text{SiO}_x$  overcoatings on some of the mirrors, and the 6  $\mu\text{m}$  structure from  $\text{H}_2\text{O}$  in the sphere

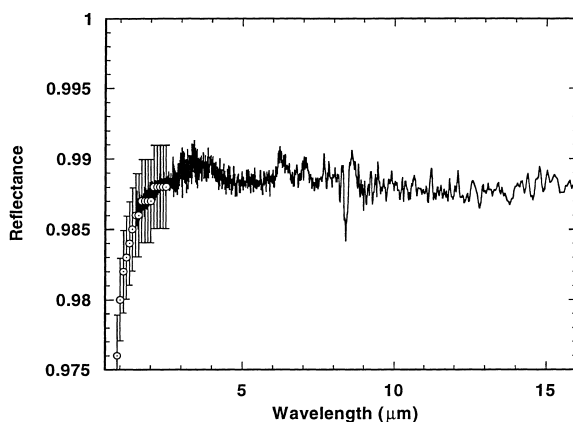


Fig. 6. Comparison of reflectance of Au SRM mirror measured on the integrating sphere with FT-IR (solid line) and the NIST STARR monochromator facility (circles).

wall. These Au mirror standard reference materials (SRMs) may possibly be extended for use as mid-IR reflectance standards.

### 2.3. *T/R measurements with goniometer*

Another method for measuring absolute reflectance is the goniometer arrangement shown in Fig. 1. In this set up, the beam is reflected from the sample directly onto the detector. Then, the sample is moved out of the beam and the detector is rotated to collect the undeflected beam. The ratio of these two measurements yields the sample reflectance. In this configuration, the angle of incidence on the sample can be varied from  $7.5^\circ$  to nearly grazing incidence (depending on the size of the sample), with a roughly  $f/20$  beam geometry.

We have performed absolute reflectance measurements with this device and have found that the difficulty in aligning the reflected beam and reference beam onto the detector (1–2 mm pyroelectric or photoconductive element) limits the relative uncertainty that can be achieved to ca. 3–5%. The use of larger, more uniform detectors should greatly decrease the alignment sensitivity and make more accurate measurements possible.

By using a HeNe alignment laser, it is possible to perform fairly accurate *relative* reflectance measurements by aligning the sample front surface and a reference mirror to within ca. 0.5 mrad of each other. The reference mirror reflectance is measured on the integrating sphere as described in Section 2.2. Using this configuration, we are able to make reflectance measurements to within 0.5–1% relative uncertainty. The advantages of the goniometer system even for near-normal  $T$  and  $R$  measurements include complete

control of the beam polarization state, greater flexibility in sample handling, and control of the sample temperature with the optical access cryostat.

Fig. 7 shows measurements of  $T$  and  $R$  for a 2 mm thick  $z$ -cut  $\text{Al}_2\text{O}_3$  disk at 296 K and 582 K, in the region of the multiphonon absorption edge for this material [18]. The measured values are compared to calculated  $T$  and  $R$  values using the OPTIMATR code [14] for the  $\text{Al}_2\text{O}_3$  dielectric function. The measured and calculated values agree quite closely except in the 6–6.5  $\mu\text{m}$  region, where the data show an absorption feature believed to be due to a 2-phonon process which is not included in the model. The relative expanded uncertainty in the measured values is estimated to be  $\pm 1\%$ .

The goniometer system incorporates high-quality Brewster's angle polarizers on the input and output arms. These polarizers have an extinction ratio of less than  $10^{-5}$  over the entire IR region [19] and can be used for highly accurate polarimetric or ellipsometric measurements, as well as the calibration of other polarizers. Fig. 8 shows the measured extinction ratios (defined as the ratio of minor to major principal transmittances) of three different IR wire grid polarizers on ZnSe substrates. The extremely low extinction ratio of the Ge chevron polarizers allows measurements such as these to be performed directly, by simply rotating the polarizer under test. This method is simpler and less prone to error than the conventional method of measuring three or more polarizers in pairs and solving a system of equations to derive the extinction ratios of the individual

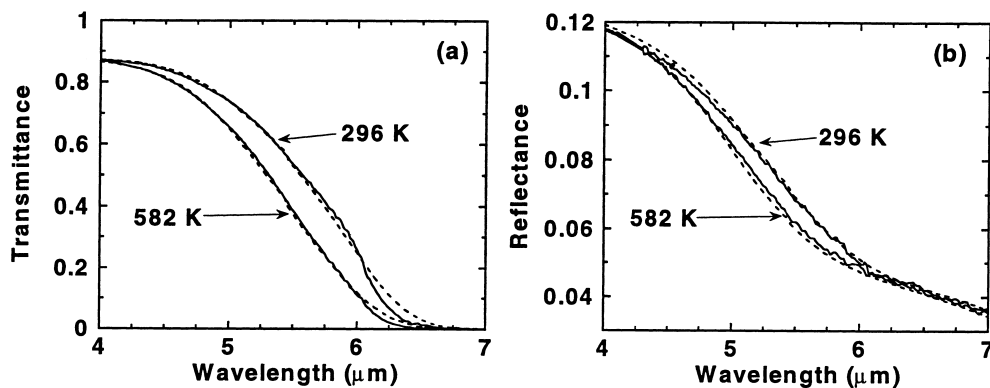


Fig. 7. Transmittance and reflectance of a 2 mm thick  $\text{Al}_2\text{O}_3$  sample measured with the goniometer system at 296 K and 582 K. The solid curves show the experimental data and the dashed curves the predicted  $T$  and  $R$  using a multiphonon model for  $\text{Al}_2\text{O}_3$ .

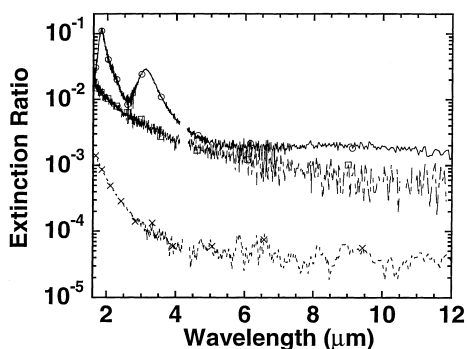


Fig. 8. Extinction ratios of three different wire grid/ZnSe polarizers measured with the goniometer system and Ge chevron polarizer.

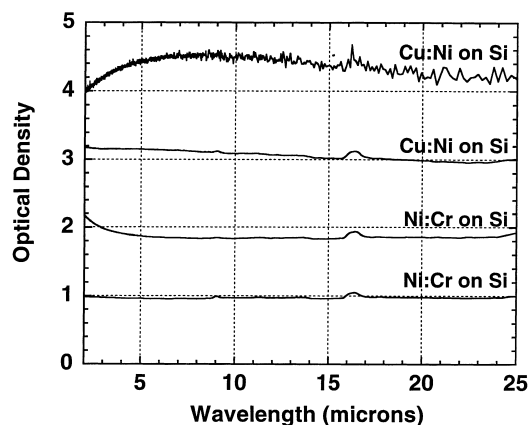


Fig. 9. Spectra for neutral density filter SRMs.

polarizers. As shown in Fig. 1,  $\text{MgF}_2$  pseudo-zero-order waveplates can also be placed in the optical train to realize a rotating-retarder polarimeter [20], which has been used to measure the complete Mueller matrix of wire-grid polarizers in the near IR (1–2  $\mu\text{m}$ ), where these polarizers have significant retardance.

### 3. Standard reference materials for regular infrared transmittance

Standard reference materials (SRMs) for IR transmittance have been developed, consisting of thin metallic (Ni:Cr or Cu:Ni) coatings on 0.25 mm thick, 25 mm diameter high-resistivity Si wafers. The coatings were designed to give nominally neutral attenuation with optical densities near 1, 2, 3, and 4 over a wavelength range of 2–25  $\mu\text{m}$ . The thin substrates were chosen to both minimize the Si absorption peaks at 9 and 16  $\mu\text{m}$ , and the effects on the geometry of the transmitted beam.

A plot of the optical density of representative samples for the four OD levels is shown in Fig. 9. As is evident in this figure, the OD 1 samples have very neutral attenuation versus wavelength, but the spectral variation is larger for the higher OD samples, with the OD 4 filters having a total variation of about 0.6 over the measured range. A comparison of the spectra of these filters with previous commercially available filters has been presented [21], and a patent has been issued for the Cu:Ni coatings [22], which

provide much more neutral attenuation at the OD 3 and 4 level than do Ni:Cr coatings.

A set of 10 samples for each OD level has been produced and the filters have been measured to determine the repeatability and reproducibility of the transmittance over a period of 6 months. The metal coatings have been overcoated with 20 nm of  $\text{SiO}_x$  to protect the films from oxidation, and it has been found that the transmittance of the samples is stable within the resolution of the measurements over the 6 month time period. Additional measurements have been performed to determine the spatial uniformity over the central 10 mm diameter circle and temperature dependence of the filters. Table 1 shows estimates for the various uncertainty components in the measured transmittances for the OD 1–4 filters, along with the expanded uncertainties at 10.6  $\mu\text{m}$  wavelength.

### 4. Conclusions

Facilities have been developed in the Optical Technology Division at NIST for measuring regular IR transmittance and reflectance with high accuracy, using specialized accessories in conjunction with commercial FT-IR spectrometers, as well as laser systems at specific wavelengths. Transmittances as low as  $10^{-6}$  can be measured with the FT-IR systems. The most accurate  $T$  and  $R$  measurements are performed with an integrating sphere, with which specular samples having  $T$  and  $R$  in range of 1–100% can be measured with relative uncertainties of 0.2–0.3%

Table 1  
Uncertainty estimates for ND filter transmittances, in % of measured values

Uncertainty source	OD 1	OD 2	OD 3	OD 4
<i>Type B</i>				
Inter-reflections	0.2	0.3	0.3	0.3
Detector non-linearity	0.1	0.1	0.05	0.05
Detector non-equivalence	0.2	0.2	0.1	0.1
Non-source emission	0.15	0.15	0.15	0.15
Beam non-uniformity	0.2	0.2	0.2	0.2
Beam displacement, deviation, focus shift	0.1	0.1	0.1	0.1
Beam-geometry, polarization	0.2	0.2	0.2	0.2
Sample vignetting	0.03	0.03	0.03	0.03
Sample scattering	0.02	0.02	0.02	0.02
Phase errors	0.1	0.1	0.1	0.1
Sample non-uniformity	0.3	0.4	3.5	4.0
Sample temperature	0.05	0.05	0.05	0.05
Sample aging	0.2	0.2	0.2	0.2
Quadrature sum	0.59	0.68	3.5	4.0
<i>Type A</i>				
Relative standard uncertainty in mean at 10.6 $\mu\text{m}$	0.2	0.2	0.5	2.0
Relative expanded uncertainty at 10.6 $\mu\text{m}$	1.2	1.4	8.1	9.0

depending on the type of the sample. A goniometer system has also been constructed and used for angle, polarization, and temperature dependent measurements. A set of neutral density filters has been produced to serve as regular transmittance standards for 2–25  $\mu\text{m}$ .

## References

- [1] L.M. Hanssen, *Appl. Opt.* (1998), submitted.
- [2] Z.M. Zhang, L.M. Hanssen, R.U. Datla, H.D. Drew, *Int. J. Thermophys.* 17 (1996) 1441.
- [3] J.R. Birch, F.J.J. Clarke, *Spectrosc. Eur.* 7 (1995) 16–22.
- [4] H.W.H.M. Jongbloets, M.J.H. Van de Steeg, E.J.C.M. Van der Werf, J.H.M. Stoelinga, P. Wyder, *Infrared Phys.* 20 (1980) 185–192.
- [5] M. A. Ford, in: C. Burgess, K.D. Mielenz (Eds.), *Advances in Standards and Methodology in Spectrophotometry*, Elsevier, Amsterdam, 1987, pp. 359–366.
- [6] D.B. Chase, *Appl. Spectrosc.* 38 (1984) 491–494.
- [7] M.I. Flik, Z.M. Zhang, *J. Quant. Spectrosc. Radiat. Transfer* 47 (1992) 293–303.
- [8] J.R. Birch, E.A. Nicol, *Infrared Phys.* 27 (1987) 159–165.
- [9] D.B. Tanner, R.P. McCall, *Appl. Opt.* 23 (1984) 2363–2368.
- [10] S.G. Kaplan, L.M. Hanssen, R.U. Datla, *Appl. Opt.* 36 (1997) 8896.
- [11] Z.M. Zhang, L.M. Hanssen, R.U. Datla, *Opt. Lett.* 20 (1995) 1077–1079.
- [12] L.M. Hanssen, S.G. Kaplan, *Microch. Acta.*, accompanying article.
- [13] E.D. Palik, *Handbook of Optical Constants of Solids*, Academic Press, Orlando, FL, 1985.
- [14] OPTIMATR 2.1, Johns Hopkins University, Applied Physics Laboratory and ARSoftware, Landover, 1993.
- [15] J.T. Cox, G. Hass, W.R. Hunter, *Appl. Opt.* 14 (1975) 1247.
- [16] J.J. Clarke, *SPIE* 2776, (1996) 184.
- [17] P.Y. Barnes, E.A. Early, A.C. Parr, *Spectral Reflectance*, NIST Special Publication 250-48, US Government Printing Office, Washington, DC, 1998.
- [18] S.G. Kaplan, L.M. Hanssen, *Emission of coated sapphire windows*, in: *Proceedings of the Seventh DOD Electromagnetic Windows Symposium*, 1998.
- [19] D.J. Dummer, S.G. Kaplan, L.M. Hanssen, A.S. Pine, Y. Zong, *Appl. Opt.* 37 (1998) 1194.
- [20] R. Chipman, *Polarimetry*, in: M. Bass (Ed.), *Handbook of Optics 2*, Chapter 22, McGraw-Hill, New York, 1995.
- [21] Z.M. Zhang, R.U. Datla, L.M. Hanssen, *Mat. Res. Soc. Symp. Proc.* 374 (1995) 117.
- [22] Z.M. Zhang, R.U. Datla, L.M. Hanssen, US Patent 5 726 797 (1998).